Process Biochemistry 99 (2020) 9–20

Contents lists available at ScienceDirect

Process Biochemistry

journal homepage: www.elsevier.com/locate/procbio

Synthesis of ethyl (*R*)-4-chloro-3-hydroxybutyrate by immobilized cells using amino acid-modified magnetic nanoparticles

Yuan Lu[a], Hongqian Dai[a], Hanbing Shi[b], Lan Tang[a], Xingyuan Sun[b,*], Zhimin Ou[a,*]

[a] College of Pharmaceutical Science, Zhejiang University of Technology, Hangzhou, Zhejiang, China
[b] The Third Affiliated Hospital of Qiqihar Medical College, Qiqihar, Heilongjiang, China

ARTICLE INFO

Keywords:
Amino acid-modified magnetic nanoparticles
Alternating magnetic field
Asym-metric reduction
Ethyl (*R*)-4-chloro-3-hydroxybutyrate
Immobilized cells

ABSTRACT

Fe_3O_4-Arg was selected as the optimal carrier due to its high activity recovery of immobilized cells in the preparation of Fe_3O_4-Arg-Cells. The optimal immobilization conditions for the preparation of Fe_3O_4-Arg-Cells were 30 °C, 4 h, pH 7, and 3 g dry yeast. The activity recovery of immobilized cells reached 76.8 %. For a batch reduction in a shaker in an alternating magnetic field, Fe_3O_4-Arg-Cells were used as a catalyst to gain ethyl (*R*)-4-chloro-3-hydroxybutyrate ((*R*)-CHBE). For further improvement in reduction productivity, a continuous reduction in the magnetic fluidized bed reactor system (MFBRS) was completed. Under their optimal transformation conditions, it took 24 h for Fe_3O_4-Arg-Cells to complete the conversion of ethyl 4-chloro-3-oxobutanoate (COBE) (0.8553 mol/L) in the shaker and only 8 h for the batch reduction in an alternating magnetic field. Continuous reduction in MFBRS provided new ideas for the efficient production of (*R*)-CHBE; 1.5882 mol/L (10 mL) of COBE can be completely converted in 6 h. The conversion and enantiomeric excess (e.e.) of (*R*)-CHBE were 100 % and above 99.9 % respectively, in the three reaction systems mentioned above.

1. Introduction

(*R*)-CHBE, an optically active alcohol, is a key intermediate for the production of chiral drugs [1,2], including L-carnitine [3], (−) macrolactin A, (*R*)-γ-amino-β-hydroxybutyric acid (GABOB) [4] and (*R*)-4-hydroxy-pyrrolidone [4,5]. Although various biocatalysts have been found to give (*S*)-CHBE, the opposite enantiomer of (*R*)-CHBE, with excellent enantioselectivity and high yields [6–9]. However, few biocatalysts that could synthesize (*R*)-CHBE with high enantioselectivity have been reported. Several biocatalysts are known to convert ethyl 4-Chloro-3-oxobutanoate (COBE) to (*R*)-CHBE including gox2036 from *Gluconobacter oxydans* [10], AKRs from *Sporobolomyces salmonicolor* [11], LEK from *Lodderomyces elongisporus* [12], a reductase from *Bacillus* sp. ECU0013 [13] and *Burkholderia gladioli* [14]. (*R*)-CHBE (100 % e.e.) was produced by Gox2036 obtained from *G. oxydans* with > 99 % conversion and 96.9 % yield (968.6 mg/L) [10]. LEAKR50 obtained from *S. salmonicolor* could completely transform 20 mM COBE to (*R*)-CHBE (98 % e.e.) [11]. The molar conversion yield of COBE was 78.0 % using LEK from *L. elongisporus*, and the e.e. value of (*R*)-CHBE was > 99 % [12]. Thus, great efforts have been made to explore more robust biocatalyst, select appropriate reaction medium and immobilize the enzyme and whole-cell to increase the reuse times of catalyst.

Much work has been done in finding a more robust biocatalyst. *E. coli* CCZU-A13 [15], E.coli BL21(DE3)pLysS (pETDuet-gaccr-gdh) [16], and a novel alcohol dehydrogenase from *Lactobacillus curieae* S1L19 [17] were adopted in the asymmetric reduction of COBE to synthesize (*R*)-CHBE for improving catalytic efficiency and stereoselectivity. An appropriate reaction medium is beneficial to prepare (*R*)-CHBE efficiently. Traditional aqueous phase [16], organic phase, water/oil system [18], and an ionic liquid [Bmim]PF6-hydrolyzate media [15] were also reported in the biotransformation of COBE to obtain (*R*)-CHBE. The conversion is low in the aqueous phase because the enzyme and whole cell have substantial catalytic activity in water and because several organic substrates are difficult to dissolve in water. A biocatalyst in the organic phase or water/oil system is used to enhance the reaction because the organic substrate readily dissolves in the organic phase, and certain enzymes and whole cells still retain activity in organic solvents or at the oil-water interface [19]. The addition of the ionic liquid and auxiliary reagent contribute to enhancement of the cell permeability and increase of mass transfer rate and conversion [15]. Meanwhile, immobilization of the enzyme and whole cell has the advantage of reusing the biocatalyst, which improves production efficiency.

In recent years, Fe_3O_4 magnetic nanoparticles (MNPs) are dramatic materials showing great performance in the immobilization of biocatalysts [20–24]. Compared with other nanoparticles, such as terracotta

* Corresponding authors.
E-mail addresses: 708900599@qq.com (X. Sun), oozzmm@163.com (Z. Ou).

https://doi.org/10.1016/j.procbio.2020.07.027
Received 21 April 2020; Received in revised form 11 July 2020; Accepted 30 July 2020
Available online 26 August 2020
1359-5113/

beads, coconut bract, corncob, Ca-alginate beads, and straw-alginate beads, Fe_3O_4 MNPs have unique properties, including the smaller core size, larger surface area for functionalization, higher coercive force, stronger surface adsorption ability, better suspension property, superparamagnetic behavior, and low toxicity. Fe_3O_4 MNPs have the remarkable characteristic of superparamagnetism, which is essential and critical for reaction in the magnetic field. Moreover, Fe_3O_4 MNPs can be easily separated and effectively recycled under an external magnetic field. Numerous varieties of cells have been successfully modified by MNPs to construct immobilized cells [25–28]. Immobilized cells are economically available biocatalysts widely applied in continuous bioprocesses currently. MNPs can be modified by biomolecules capable of selectively interacting with surface groups of cells to form functionalized MNPs, which could efficiently capture the cells. However, many such biomolecules are large molecules that would decrease the amount anchored onto the MNPs surface and therefore affect the cell immobilization efficiency. Jin et al. [29] used three strong positive charged amino acids, arginine (Arg), lysine (Lys) and poly-L-lysine (PLL) to modify MNPs through a simple and economical two-step transformation process (TST) for bacteria capture and removal. Modification of Fe_3O_4 nanoparticles with amino acids greatly enhanced the bacteria capture efficiency and kinetics towards both Gram-positive *B. subtilis* and Gram-negative *E. coli*. For both bacterial cells, the three amino acid-functionalized Fe_3O_4 particles (Fe_3O_4-AA) types could capture more than 97 % of the bacterial cells in 20 min. Cell capture by Fe_3O_4-AA is governed by energy interactions between cells and nanoparticle surface. These interactions mainly include van der Waals forces and electrostatic double-layer repulsion. In addition, hydrophobic interaction and hydrogen bonding might be involved [29].

In this study, *Saccharomyces cerevisiae* CGMCC No. 3361, which is highly capable of asymmetric reduction of COBE, was selected. Amino acids are desirable chemicals as ligands anchored with MNPs. Two positively charged polar amino acids (arginine, lysine) and two negatively charged polar amino acids (glutamate, aspartic acid) were used in the modification of MNPs. A facile and inexpensive process was applied in the preparation of four types of Fe_3O_4-AA. Fe_3O_4-AA-Cells were prepared by the efficient immobilization of *S. cerevisiae* CGMCC No. 3361 on Fe_3O_4-AA. (*R*)-CHBE was synthesized by asymmetric reduction of COBE with Fe_3O_4-AA-Cells in a shaker in an alternating magnetic field. Both carbonyl reductase and NADPH were present in cells. Carbonyl reductase catalyzed the asymmetric reduction of COBE to (*R*)-CHBE. NADPH served as the hydrogen donor for reduction. The mechanism of asymmetric reduction of COBE is shown in Fig. 1.

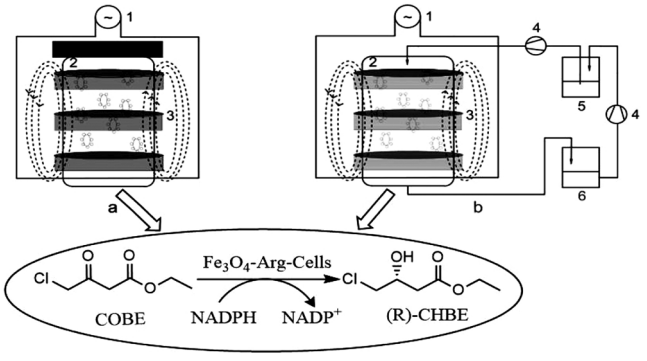

Fig. 1. Batch (a) and continuous (b) reduction reaction in an alternating magnetic field (Fe_3O_4-Arg-Cells, 1 Alternating current power supply, 2 Reactor, 3 Helmholtz coil, 4 Constant flow pump, 5 Inflow tank, 6 Effluent tank).

2. Materials and method

2.1. Materials

Ferric chloride hexahydrate ($FeCl_3$•$6H_2O$), ferrous sulfate heptahydrate ($FeSO_4$•$7H_2O$), L-arginine powder (98 %), L-lysine powder (99 %), L-glutamate powder (99 %) and L-aspartic acid powder (98 %) were purchased from Shanghai Aladdin Bio-Chem Technology Co., Ltd. Ethyl 4-chloro-3-oxobutanoate (99 %) standard was purchased from Bangcheng Chemical Co., Ltd. Shanghai, China. (*S*)-CHBE and (*R*)-CHBE standard were purchased from Aladdin reagent Co., Ltd. Shanghai, China. *S. cerevisiae* CGMCC No. 3361 was preserved in China General Microbiological Culture Collection Center.

2.2. Analytical methods

The activity recovery of immobilized cells was analyzed by spectrophotometer. The cell solution without Fe_3O_4-AA carrier was used as a reference solution. The ultraviolet absorption (A_0) at a wavelength of 260 nm of the cell solution diluted twenty times was used as the initial concentration. The absorption of the supernatant liquid after immobilization was taken as the A_i. The activity recovery of immobilized cells (*AD*) was calculated by Eq. (1):

$$AD = \frac{A_0 - A_i}{A_0} \times 100\% \quad (1)$$

The conversion and enantiomeric excess of (*R*)-CHBE were analyzed using a Shimadzu GC-2014 gas chromatograph. The conversion was defined as the ratio of the converted substrate concentration to the initial substrate concentration. The enantiomer excess of CHBE was detected by the derivatization method. At the end of reduction, the catalyst was recovered by an external magnetic field. 4 mL of ethyl acetate was added in a stoppered test tube containing 11 mL of the supernatant. 1 mL of ethyl acetate extract was adopted in a glass bottle for the derivatization reaction (natural volatile solvent at room temperature, then 2 drops of acetic anhydride and 2 drops of pyridine were added in a fume hood and placed in a boiling water bath for 1 h). After slightly cooling, 1 mL of ethyl acetate was used to dilute the above sample. The sample was analyzed by GC equipped with a Agilent CP7502 J&W CP-CHirasil-Dex CB chiral column (Machery-Nagel; 25 m × 0.25 mm × 0.25 mm). Injector, column and FID temperature were 250, 110 and 250 ℃. H_2 pressure: 83 kPa. Split ratio: 1:15. Retention time of COBE, (*S*)-CHBE and (*R*)-CHBE were 10.107, 20.035 and 21.000 min. Eqs. (2) and (3) evaluated the conversion (X) and enantiomeric excess of CHBE.

$$X(\%) = \frac{P \times Ms}{Q \times Mp} \times 100\% \quad (2)$$

Ms and *Mp* are the molecular weight of the substrate and the product. *P* and *Q* stand for the mass of the product at the end of the reaction and the initial mass of the substrate.

$$ee_p = \frac{C_R - C_S}{C_R + C_S} \times 100\% \quad (3)$$

C_R and C_S stand for the concentration of (*R*)-CHBE and (*S*)-CHBE.

2.3. Preparation of yeast cell lyophilized powder

The solid medium comprised of wort 10 g/L, yeast powder 3 g/L, peptone 5 g/L, glucose 10 g/L, agar 20 g/L. The liquid medium consisted of glucose 30 g/L, yeast powder 3 g/L, ammonium sulfate 5 g/L, $MgSO_4$ 0.3 g/L, K_2HPO_4•$3H_2O$ 1 g/L, KH_2PO_4 1 g/L. *S. cerevisiae* CGMCC No. 3361 was inoculated into a solid medium and cultured at 30 ℃ for 5 days to obtain a yeast colony. A loop of yeast colony was transferred into the liquid medium. After cultivation in liquid medium at 35 ℃ for 15 h, a seed liquid was obtained. The seed liquid was

inoculated into the liquid medium at a seed volume of 10 % for fermentation. The fermentation broth was obtained after cultivation at 35 ˚C, 150 r/min for 24 h. Then, the fermentation broth was centrifuged and the precipitate harvested. The lyophilized powder of *S. cerevisiae* 3361 was obtained after the precipitate was frozen at −80 ˚C for 8 h and lyophilized in a freeze dryer for 12 h.

2.4. Preparation of Fe_3O_4, Fe_3O_4-AA, and Fe_3O_4-AA-Cells

Magnetic Fe_3O_4 nanoparticles were prepared. 0.03 M $FeCl_3$•$6H_2O$ (40 mL) and 0.02 M $FeSO_4$•$7H_2O$ (40 mL) solutions were mixed with a mechanical stirrer in a 250 mL flask containing 150 mL of deionized water. This solution was chemically precipitated at 40 ℃ by adding NH_3•H_2O dropwise until the pH reached 10. The above processes needed vigorous stirring with nitrogen protection. The suspension was heated to 80 ℃ for 1 h with continuous stirring. A black precipitate was formed under the above conditions and was cooled at 20–30 ℃. The black precipitate was collected by magnetic decantation and washed with deionized water repeatedly until the washings were neutral. The obtained black precipitates were pre-frozen in a -80 ℃ refrigerator for 8 h and then lyophilized in a freeze dryer for 12 h to obtain magnetic Fe_3O_4 nanoparticles.

Fe_3O_4-AA including Fe_3O_4-Arg, Fe_3O_4-Lys, Fe_3O_4-Glu, and Fe_3O_4-Asp was prepared. 0.1 g magnetic Fe_3O_4 nanoparticles were added in 100 mL of the corresponding amino acid solution (0.1 g/100 mL) under ultrasonication for 30 min. After the sonication treatment, the obtained black precipitates were collected with magnetic decantation and washed with deionized water three times. Fe_3O_4-AA was obtained after being frozen for 8 h in a −80 ℃ refrigerator and lyophilized in a freeze dryer for 12 h.

Fe_3O_4-AA-Cells were prepared. The yeast cell lyophilized powder was dispersed in 20 mL of 0.1 mol/L phosphate-buffered saline solution. Fe_3O_4-AA was added to the above solution. The mixture was shaken at 30 ℃, 150 r/min. After 3–4 h, Fe_3O_4-AA-cells were collected by an external magnetic field and washed with deionized water until the upper layer had no ultraviolet absorption at a wavelength of 260 nm. Fe_3O_4-AA-cells were frozen at −80 ˚C for 8 h and lyophilized in a freeze dryer for 12 h.

2.5. Optimization of immobilized condition and selection of optimal Fe_3O_4-AA-Cells for asymmetric reduction of COBE

To find an excellent Fe_3O_4-AA-Cells for asymmetric reduction of COBE, the effects of immobilized conditions on activity recovery of immobilized cells were studied during the preparation of four kinds of Fe_3O_4-AA-Cells. Fe_3O_4-AA-Cells were collected by an external magnetic field. The remaining liquid in the flask was analyzed to determine the activity recovery of immobilized cells. Furthermore, Fe_3O_4-Arg-Cells, Fe_3O_4-Glu-Cells, Fe_3O_4-Lys-Cells, and Fe_3O_4-Asp-Cells were prepared under optimal conditions and used in the asymmetric reduction of COBE to select the optimal Fe_3O_4-AA-Cells.

2.5.1. Effect of time on the activity recovery of immobilized cells

0.03 g Fe_3O_4-Arg was added in five conical flasks containing a 0.15 g/mL yeast cell solution (20 mL, pH 7) at 30 ℃, 150 r/min shaker for 2 h, 3 h, 4 h, 5 h, and 6 h, respectively. The immobilization processes of other carriers of Fe_3O_4-AA were analogous except for the concentration of the yeast cells. The cell concentrations corresponding to the carrier Fe_3O_4-Glu, Fe_3O_4-Lys and Fe_3O_4-Asp were 0.075 g/mL, 0.15 g/mL, and 0.15 g/mL, respectively.

2.5.2. Effect of temperature on the activity recovery of immobilized cells

0.03 g Fe_3O_4-Arg was added in five conical flasks containing a 0.15 g/mL yeast cell solution (20 mL, pH 7) at 20 ℃, 25 ℃, 30 ℃, 35 ℃, and 40 ℃, 150 r/min shaker for 4 h respectively. The immobilization processes of other carriers were analogous except the immobilization conditions were slightly different. The cell concentration corresponding to the carrier Fe_3O_4-Glu was 0.075 g/mL, while Fe_3O_4-Lys and Fe_3O_4-Asp were 0.15 g/mL. The immobilization time was 3 h for Fe_3O_4-Lys and Fe_3O_4-Glu.

2.5.3. Effect of Fe_3O_4-AA amount on the activity recovery of immobilized cells

0.01 g, 0.015 g, 0.02 g, 0.025 g, and 0.03 g Fe_3O_4-AA were added into five conical flasks containing a yeast cell solution (20 mL, pH 7). The biomass was 0.075 g/mL for Fe_3O_4-Glu, while the biomass was 0.15 g/mL for Fe_3O_4-Arg, Fe_3O_4-Lys, and Fe_3O_4-Asp, respectively. The immobilization process was carried out at 30 ℃, 150 r/min. The reaction time was 3 h for Fe_3O_4-Lys and Fe_3O_4-Glu, while the reaction time was 4 h for Fe_3O_4-Arg and Fe_3O_4-Asp.

2.5.4. Effect of initial free cell concentration on the activity recovery of immobilized cells

0.03 g Fe_3O_4-AA was added to five conical flasks containing 0.050 g/mL, 0.075 g/mL, 0.100 g/mL, 0.125 g/mL, and 0.150 g/mL of a yeast cell solution (20 mL, pH 7), respectively. The immobilization process was carried out at 30 ℃, 150 r/min shaker. The immobilization time was 4 h for Fe_3O_4-Arg or Fe_3O_4-Asp, while the immobilization time was 3 h for Fe_3O_4-Glu and Fe_3O_4-Lys.

2.5.5. Selection of optimal Fe_3O_4-AA-Cells for asymmetric reduction of COBE

Four kinds of Fe_3O_4-AA-Cells were prepared under the optimization conditions. The optimal Fe_3O_4-AA-Cells were selected by comparison of reduction conversion.

2.6. Characterization of Fe_3O_4, optimal Fe_3O_4-AA, and Fe_3O_4-AA-Cells

The FT-IR spectra of Fe_3O_4, optimal Fe_3O_4-AA, and Fe_3O_4-AA-Cells were obtained using an FT-IR spectrophotometer (iS50, Nicolet). The surface features of Fe_3O_4, optimal Fe_3O_4-AA, and Fe_3O_4-AA-Cells were evaluated by a field emission scanning electron microscope (SEM) (Zeiss Gemini 500). The content of elements in the samples were determined by energy dispersive X-Ray spectroscopy (EDX) (XFlash 6/60, Bruker). Fe_3O_4, optimal Fe_3O_4-AA, and Fe_3O_4-AA-Cells were analyzed by X-ray powder diffraction (XRD). XRD measurements were conducted on a Rigaku D/MAX-3B X-ray diffractometer employing Cu Kα radiation (λ = 0.1542 nm).

2.7. Optimization of the batch reduction conditions in a shaker

The effects of conditions on reduction were investigated. At the end of the reaction, the conversion and enantiomeric excess of CHBE were determined by the analytical methods used in Section 2.2.

2.7.1. Effect of reaction time on reduction

2.334 g of Fe_3O_4-Arg-Cells were dispersed in 10 mL of 0.1 mol/L phosphate-buffered saline (pH 9) in five 50 mL small conical flasks. 9.408 mol/L of COBE ethanol solution (1 mL) was added in the flask. The concentration of COBE in reaction mixture was 0.8553 mol/L. The flask was shaken at 35 ℃, 150 r/min for 16 h, 24 h, 32 h, 40 h, and 48 h, respectively.

2.7.2. Effect of substrate concentration on reduction

2.334 g of Fe_3O_4-Arg-Cells were dispersed in 10 mL of 0.1 mol/L phosphate-buffered saline (pH 9) in five 50 mL small conical flasks. 1 mL of COBE ethanol solution (1.344 mol/L, 4.032 mol/L, 6.72 mol/L, 9.408 mol/L, and 12.096 mol/L) was added into 10 mL of 0.1 mol/L phosphate-buffered saline (pH 9). The concentration of COBE in reaction mixture were 0.1222 mol/L, 0.3665 mol/L, 0.6109 mol/L, 0.8553 mol/L, and 1.0996 mol/L. The reduction was carried out at 35 ℃, 150 r/min for 24 h.

2.7.3. Effect of temperature on reduction

2.334 g of Fe_3O_4-Arg-Cells were dispersed in 10 mL of 0.1 mol/L phosphate-buffered saline (pH 9) in five 50 mL small conical flasks. 9.408 mol/L of COBE ethanol solution (1 mL) was added into the mixture. The concentration of COBE in reaction mixture was 0.8553 mol/L. The reduction was carried out at different temperatures (20 ℃, 25 ℃, 30 ℃, 35 ℃, 40 ℃), 150 r/min for 24 h.

2.7.4. Effect of pH of buffer on the reduction

2.334 g of Fe_3O_4-Arg-Cells were dispersed in 10 mL of 0.1 mol/L phosphate-buffered saline (pH 5, pH 6, pH 7, pH 8, and pH 9) in five 50 mL small conical flasks. 9.408 mol/L of COBE ethanol solution (1 mL) was added into the mixture. The concentration of COBE in reaction mixture was 0.8553 mol/L. The reduction was carried out at 35 ℃, 150 r/min for 24 h.

2.8. Reuse of Fe_3O_4-Arg-Cells in the shaker reduction

The reduction was catalyzed by Fe_3O_4-Arg-Cells under optimum conditions. 2.334 g of Fe_3O_4-Arg-Cells was dispersed in 10 mL of 0.1 mol/L phosphate-buffered saline (pH 9) in a 50 mL small conical flask. 9.408 mol/L of COBE ethanol solution (1 mL) was added into the mixture. The concentration of COBE in reaction mixture was 0.8553 mol/L. After a 24 h reduction at 35 ℃ in a 150 r/min shaker, the Fe_3O_4-Arg-Cells were recovered using an external magnetic field and washed 10 times with ethanol and deionized water to ensure that no substrate or product residue left on Fe_3O_4-Arg-Cells. Fe_3O_4-Arg-Cells was reused in the reduction and recycled under the above-mentioned reduction conditions.

2.9. Optimization of batch reduction conditions in an alternating magnetic field

2.9.1. Effect of magnetic field strength on the activity of Fe_3O_4-Arg-Cells

An alternating magnetic field was generated using a lab-made device. A schematic diagram of the device for generating an electromagnetic alternating field is illustrated in Fig. 1a. The strength and frequency of the magnetic field could be adjusted based on actual demand. The reactions were conducted in an alternating magnetic field with a specific frequency of 500 Hz for 8 h. 2.334 g of Fe_3O_4-Arg-Cells were dispersed in 10 mL of 0.1 mol/L phosphate-buffered saline (pH 9). 9.408 mol/L of COBE ethanol solution (1 mL) was added to the mixture. The concentration of COBE in reaction mixture was 0.8553 mol/L. The influence of magnetic field strength on reduction was investigated when the magnetic field strengths were 4 Gs, 8 Gs, 12 Gs, 16 Gs, and 20 Gs.

2.9.2. Effect of reaction time on reduction in an alternating magnetic field

2.334 g of Fe_3O_4-Arg-Cells were dispersed in 10 mL of 0.1 mol/L phosphate-buffered saline (pH 9) in five 30 mL reaction flasks in the apparatus shown in Fig. 2a. 9.408 mol/L COBE ethanol solution (1 mL) was added into the mixture. The concentration of COBE in reaction mixture was 0.8553 mol/L. The reaction was carried out in the alternating magnetic field at 35 ℃ for 2 h, 4 h, 6 h, 8 h, and 10 h, respectively. The reactions were conducted in an alternating magnetic field with a specific frequency of 500 Hz and magnetic field strength of 12 Gs.

2.10. Optimization of continuous reduction conditions in a magnetic fluidized bed reactor system (MFBRS)

The MFBRS consisted of a jacketed glass tube reactor (Din = 1.5 cm, H = 20 cm) and three copper wire coils, which were connected to a power supply (0–10 A, 0.1 A sensitivity) and produced an axially uniform magnetic field to prevent the escape of the magnetic particles from the bed. A set of three Helmholtz coils were evenly spaced (16 mm apart) along the vertical axis and used to generate the external magnetic fields. Each coil had a 120 mm inner diameter, 160 mm outer diameter, 20 mm thickness, and contained 600 wraps of AWG#21 copper wire [30]. The magnetic field intensity was controlled by adjusting the current, which was passed through the solenoid using a AC power supplier. A constant flow pump was used for the flow of the substrate solution through the reactor. The schematic diagram of the device is shown in Fig. 1b.

2.10.1. Effect of substrate flow rate on reduction in MFBRS

2.334 g of Fe_3O_4-Arg-Cells were dispersed in 10 mL of 0.1 mol/L phosphate-buffered saline solution (pH 9) in the reaction tank. 1.5882 mol/L of COBE ethanol solution (10 mL) was added to the mixture and a constant flow pump pumped the COBE ethanol solution in tank 5 into the reaction tank. The substrate flow rate was 25 μL/min, 30 μL/min, 40 μL/min, 50 μL/min, 100 μL/min, and 200 μL/min. The reaction mixture was pumped into the effluent tank at the same rate as the substrate flow rate. The reduction in the reactor was performed at 35 ℃, and magnetic field intensity of 12 Gs for 6 h.

2.10.2. Effect of substrate concentration on reduction in MFBRS

2.334 g of Fe_3O_4-Arg-Cells were dispersed in 10 mL of 0.1 mol/L phosphate-buffered saline solution (pH 9) in the reaction tank. 10 mL of COBE ethanol solution (0.6109 mol/L, 0.8553 mol/L, 1.0996 mol/L, 1.3439 mol/L, 1.5882 mol/L and 1.8325 mol/L) was added to the tank 5 respectively. A constant flow pump with a substrate flow rate of 25 μL/min respectively pumped the solutions in tank 5 into the reaction tank. The reaction mixture was pumped into the effluent tank at the same rate as the substrate flow rate. The reduction was performed at 35 ℃, a magnetic field intensity of 12 Gs for 6 h.

3. Results and discussion

3.1. Optimization of the preparation conditions for Fe_3O_4-AA-Cells

3.1.1. Effect of time on the activity recovery of immobilized cells

The cells are not initially completely bound to the carrier. With the prolongation of time, the active groups on the surface of the carrier were sufficiently connected with the cells to reach a saturation level. Bare Fe_3O_4 could only immobilize 11.43 % of the cells in 2 h, while the activity recovery of immobilized cells with Fe_3O_4-Arg reached 47.24 %. Although increasing the reaction time within a certain range would improve the activity recovery of immobilized cells, only 23.68 % of the cells were immobilized on bare Fe_3O_4 while 77.3 % of the cells were immobilized on Fe_3O_4-Arg within 4 h. It was evident that the modification of Fe_3O_4 with amino acids greatly enhanced the activity recovery of immobilized cells and cell capture efficiency. Fig. 2 showed that the activity recovery of immobilized cells reached the maximum value at 4 h with Fe_3O_4, Fe_3O_4-Asp, and Fe_3O_4-Arg as carriers for the cell immobilization. The optimal time was 4 h for the preparation of Fe_3O_4-Asp-Cells and Fe_3O_4-Arg-Cells. Meanwhile, the optimal time was 3 h for Fe_3O_4-Lys-Cells and Fe_3O_4-Glu-Cells formation.

3.1.2. Effect of temperature on the activity recovery of immobilized cells

A low activity recovery of immobilized cells was obtained at a low temperature (< 30 ℃) because the unit carriers were not saturated. The immobilization reaction proceeded at a faster rate with the increase of temperature. However, the activity recovery of immobilized cells decreased when the temperature reached above 30 ℃. Fig. 2 showed that the optimal immobilization temperature was 30 ℃. When the temperature was 30 ℃, all four types of Fe_3O_4-AA could immobilize more than 43 % of the cells. Particularly, the activity recovery of immobilized cells of Fe_3O_4-Arg was 77.3 %. It had a significant advantage over bare Fe_3O_4 that had an activity recovery of immobilized cells of 23.68 %. The isoelectric points of Fe_3O_4-Arg increased compared with bare Fe_3O_4 [29]. The enhanced isoelectric points of Fe_3O_4-Arg could ensure a

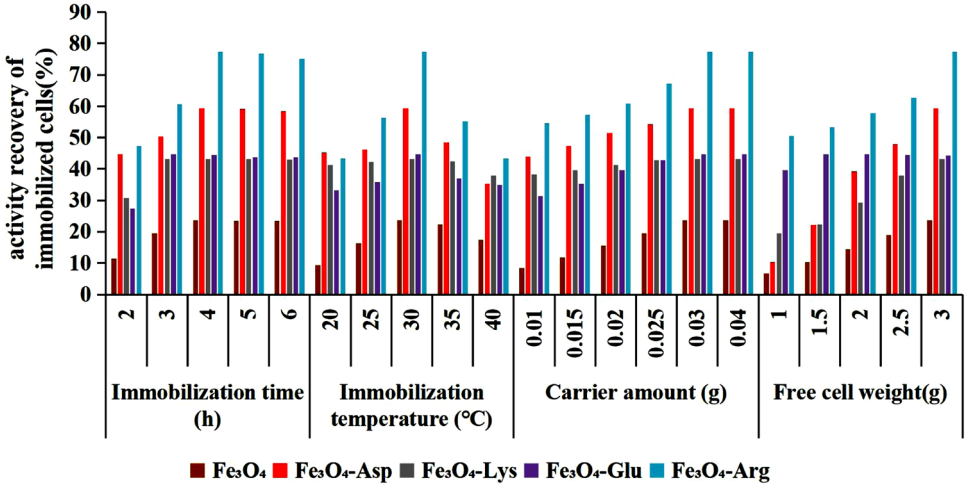

Fig. 2. Effect of immobilized condition on the activity recovery of immobilized cells.

stronger electrostatic force between nanoparticles and cells to increase activity recovery of immobilized cells [29]. Amino acids interacted with nanoparticle surface through the carboxyl groups and side chains exposed to the exterior. Fe_3O_4-Arg with side-chain functional groups also provide an active group for interaction with multiple biological molecules and ligands [31,32]. The hydrogen bonding interactions between the carboxyl oxygen of the cell membrane and the amino/imino of amino acids on the surface of Fe_3O_4-Arg nanoparticles, along with hydrophobic attractions of the carbon chains of amino acids with methyl side chains in the cell membrane, might also contribute to the activity recovery of immobilized cells by Fe_3O_4-Arg [33].

3.1.3. Effect of Fe_3O_4-AA amount on the activity recovery of immobilized cells

Due to the difference in the molecular structure of different amino acids, there is also a difference in immobilization ability between the carriers (Fe_3O_4-AA) modified by different amino acids. Fig. 2 showed that the activity recovery of immobilized cells increased with the increase of carrier amounts for bare Fe_3O_4 and the four types of Fe_3O_4-AA. In contrast with Fe_3O_4-Arg and Fe_3O_4-Asp, the activity recovery of immobilized cells of Fe_3O_4-Lys and Fe_3O_4-Glu were lower within carrier amounts from 0.01 g to 0.03 g. Fe_3O_4-Arg could provide more active binding points for cell immobilization. Fig. 2 showed that the optimal carrier amount was 0.03 g for bare Fe_3O_4 and various types of Fe_3O_4-AA. The higher activity recovery of immobilized cells was observed for Fe_3O_4-Arg.

3.1.4. Effect of initial biomass on the activity recovery of immobilized cells

The initial biomass was studied in the range of 1–3 g because the cells cannot be evenly dispersed in 20 mL of PBS when the dry weight of cells exceeds 3 g. Generally, the activity recovery of immobilized cells increased with the increase of biomass until the carriers were saturated. Fig. 2 showed that the optimal initial biomass was 1.5 g for the preparation of Fe_3O_4-Glu-Cells, while the optimal initial biomass was 3 g for the preparation of Fe_3O_4-Asp-Cells, Fe_3O_4-Arg-Cells, and Fe_3O_4-Lys-Cells. This difference may be due to the saturation of the active sites on the surface of Fe_3O_4-Glu. When the initial cell weight was 3 g, even the Fe_3O_4-Lys with the lowest activity recovery of immobilized cells among the four Fe_3O_4-AA carriers had a higher activity recovery of immobilized cells (43.26 %) than that of bare Fe_3O_4 (23.68 %).

3.1.5. Selection of optimal Fe_3O_4-AA-Cells for asymmetric reduction of COBE

The optimal conditions for the preparation of the four types of Fe_3O_4-AA-Cells were summarized in Table 1. The results showed that the maximum activity recovery of immobilized cells was obtained with Fe_3O_4-Arg as a carrier. A higher activity recovery of immobilized cells illustrated that more biomass of cells can be immobilized per unit mass carrier. Four types of Fe_3O_4-AA-Cells were prepared under their optimal preparation conditions and used in asymmetric reduction of COBE. Fig. 3 showed that conversion with Fe_3O_4-Arg-Cells as catalyst reached the optimal value compared with the other three immobilized cells (Fe_3O_4-Lys-Cells, Fe_3O_4-Glu-Cells, and Fe_3O_4-Asp-Cells). Therefore, the Fe_3O_4-Arg-Cells was selected as the optimal catalyst and used for further study.

3.2. Characterization of Fe_3O_4, Fe_3O_4-Arg, and Fe_3O_4-Arg-Cells

The FT-IR spectra of Fe_3O_4, Fe_3O_4-Arg, and Fe_3O_4-Arg-Cells in the range of $400-4000\ cm^{-1}$ were recorded and presented in Fig. 4. The characteristic absorption peak was observed at around $570-635$, 1630, and $3400\ cm^{-1}$ in FT-IR spectra. The strong absorption bands at around $570-635\ cm^{-1}$ reflect the vibration of Fe—O [29,34,35], indicating that the preparation of Fe_3O_4 was successful and Fe_3O_4 existed in the structure of Fe_3O_4-Arg and Fe_3O_4-Arg-Cells. In aqueous medium, MNP surface is modified by OH groups owing to the interaction between unsaturated surface Fe atoms and hydroxylions or water molecules. These OH groups absorb IR waves at approximately $1630\ cm^{-1}$ (deforming) and $3400\ cm^{-1}$ (stretching) [36,37]. In Fe_3O_4-Arg nanoparticles, C═O stretching vibrations are observed at $1633\ cm^{-1}$ [32]. For Fe_3O_4-Arg and Fe_3O_4-Arg-Cells, OH stretching overlaps with N—H stretching vibration at $3420\ cm^{-1}$. Similar results were reported by Antal et al. [36] and Ebrahiminezhad et al. [32].

XRD patterns of Fe_3O_4, Fe_3O_4-Arg, and Fe_3O_4-Arg-Cells were shown in Fig. 5. The six peaks (2θ of 30.1, 35.5, 43.1, 53.4, 57.0 and 62.6) were observed in the spectra of Fe_3O_4-Arg. Fe_3O_4-Arg-Cells were consistent with the six characteristic peaks observed in the pure Fe_3O_4 spectra (JCPD standards: Fe_3O_4, 89–3854, $2\theta = 30.088$, 35.439, 43.07, 53.432, 56.958, and 62.546). This indicates that the crystal form transformation did not occur during the amino acid modification processes and all three materials contained Fe_3O_4. The immobilization process did not have a destructive effect on the crystal structure of magnetite. The magnetic particles could preserve their magnetic properties during the separation process, which was beneficial for conducting bioseparation.

Fe_3O_4, Fe_3O_4-Arg, and Fe_3O_4-Arg-Cells were characterized using SEM/EDX. The results were shown in Fig. 6. It can be observed in Fig. 6(A) that the appearance of Fe_3O_4 was nearly spherical with a diameter of $10-20$ nm. Fe_3O_4 is uniform in size. The results were consistent with Unal et al's prior study [38]. After Fe_3O_4 dispersed into

Table 1
Optimal condition for the preparation of Fe_3O_4-AA-Cells.

Carriers	Time(h)	Temperature(℃)	Amount of Fe_3O_4-AA (g)	Dry yeast(g)	Weight of Fe_3O_4-AA-Cells(g)	Activity recovery of immobilized cells(%)
Fe_3O_4-Arg	4	30	0.03	3	2.334	76.8
Fe_3O_4-Lys	3	30	0.03	3	1.3078	42.59
Fe_3O_4-Glu	3	30	0.03	1.5	0.7002	44.68
Fe_3O_4-Asp	4	30	0.03	3	1.7973	58.91

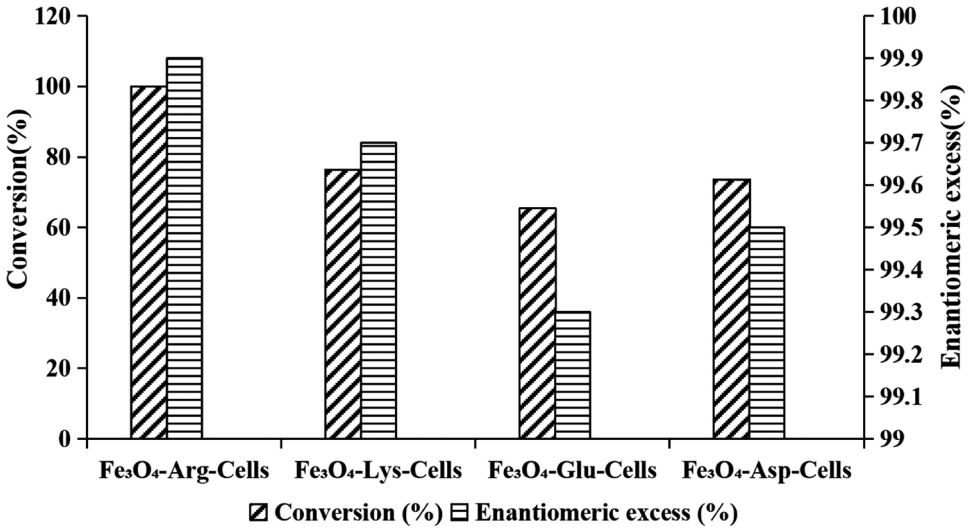

Fig. 3. Selection of optimal Fe_3O_4-AA-Cells for asymmetric reduction of ethyl 4-chloro-3-oxobutanoate (COBE). (Reduction time 24 h, 35 ℃, initial COBE concentration 0.8553 mol/L, pH 9).

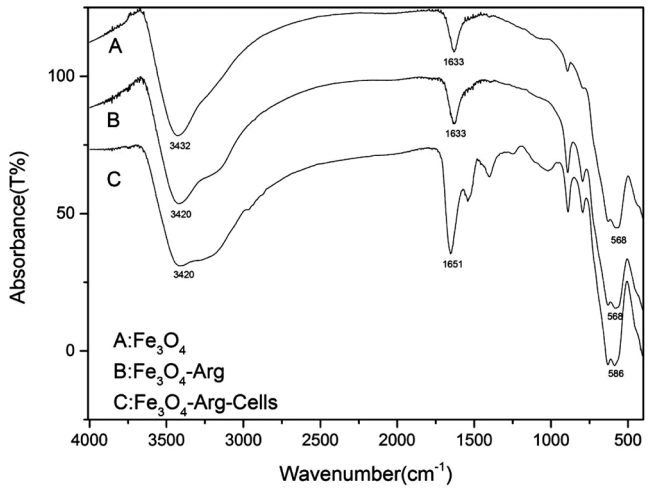

Fig. 4. FT-IR spectra of Fe_3O_4, Fe_3O_4-Arg, Fe_3O_4-Arg-Cells.

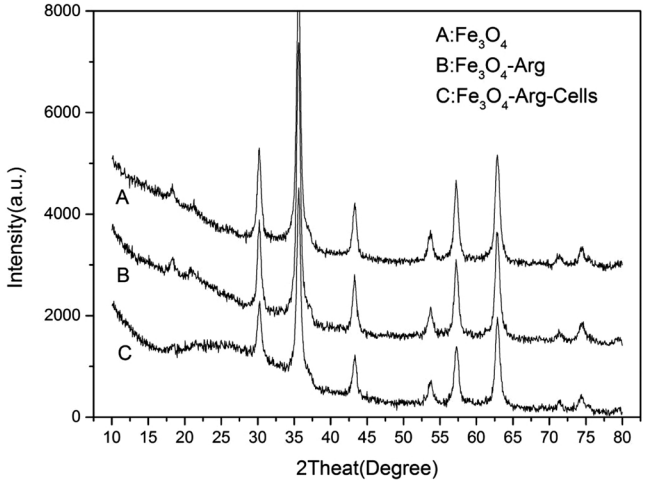

Fig. 5. XRD patterns for Fe_3O_4, Fe_3O_4-Arg, Fe_3O_4-Arg-Cells.

water, the dispersion effect was not ideal and the size of Fe_3O_4 was found to be larger. This was due to homoaggregation between the Fe_3O_4 nanoparticles because of the formation of a large number of hydrogen bonds between the surface-rich hydroxyl groups. Fig. 6(B) was the SEM/EDX image of the Fe_3O_4-Arg. From the SEM image of Fe_3O_4-Arg, near-spherical appearance was observed. The overall size of Fe_3O_4-Arg was slightly larger than that of Fe_3O_4. In the EDX spectrum of Fig. 6(B), the presence of N element provided a basis for the successful connection of arginine with Fe_3O_4 nanoparticles. It can be seen in Fig. 6(C) that some rod-like substances were attached to the surface of the spherical carrier (Fe_3O_4-Arg). According to the morphology and FT-IR spectra of Fe_3O_4-Arg-Cells, the cells were successfully immobilized on the carrier (Fe_3O_4-Arg).

3.3. Optimization of the reaction condition for asymmetric reduction of COBE

3.3.1. Effect of reaction time on reduction

Fig. 7 illustrated that the reaction time affected the conversion and enantiomeric excess of (*R*)-CHBE. COBE could be gradually converted by Fe_3O_4-Arg-Cells with a reaction time extension. The conversion increased with the increase of reaction time at < 24 h. Conversion reached 100 % at 24 h. The enantiomeric excess of (*R*)-CHBE was maintained above 99.9 %. The optimal reaction time was 24 h.

3.3.2. Effect of substrate concentration on reduction

Fig. 7 showed that conversion reached 100 % when the substrate concentration was below 0.8553 mol/L. The conversion decreased with

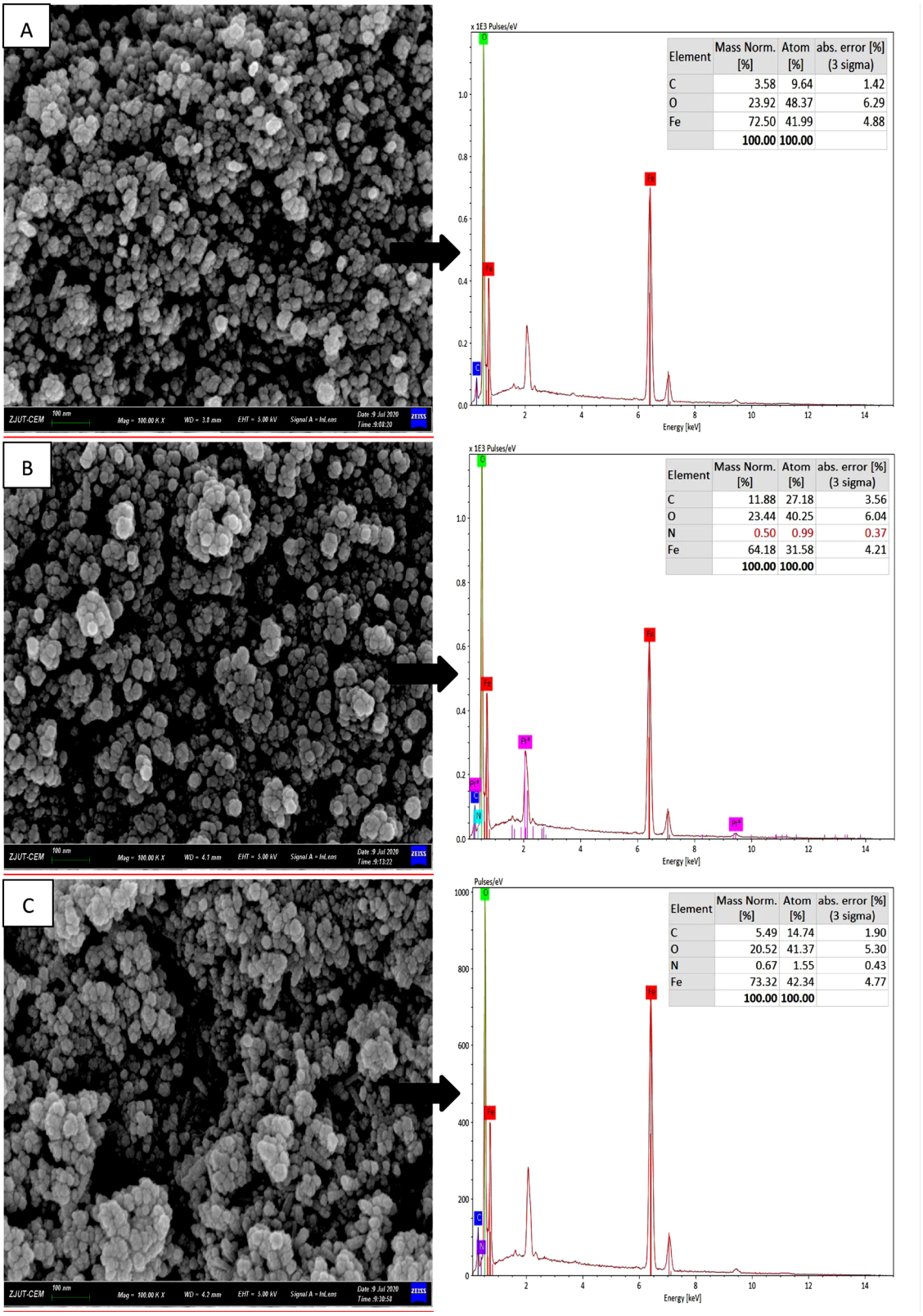

Fig. 6. SEM/EDX image of Fe_3O_4 (A), Fe_3O_4-Arg (B), Fe_3O_4-Arg-Cells (C).

the increase of substrate concentrations at above 0.8553 mol/L of COBE. At low substrate concentrations, the active site of Fe_3O_4-Arg-Cells was not fully saturated and its catalytic potential was not fully exploited. With further increases in the substrate concentration, conversion decreased slightly, possibly owing to the substrate inhibition of the Fe_3O_4-Arg-Cells activity. The presence of the carrier may have made it difficult for the substrate to contact the active site of the immobilized cells, which led to a conversion decrease at high substrate concentrations.

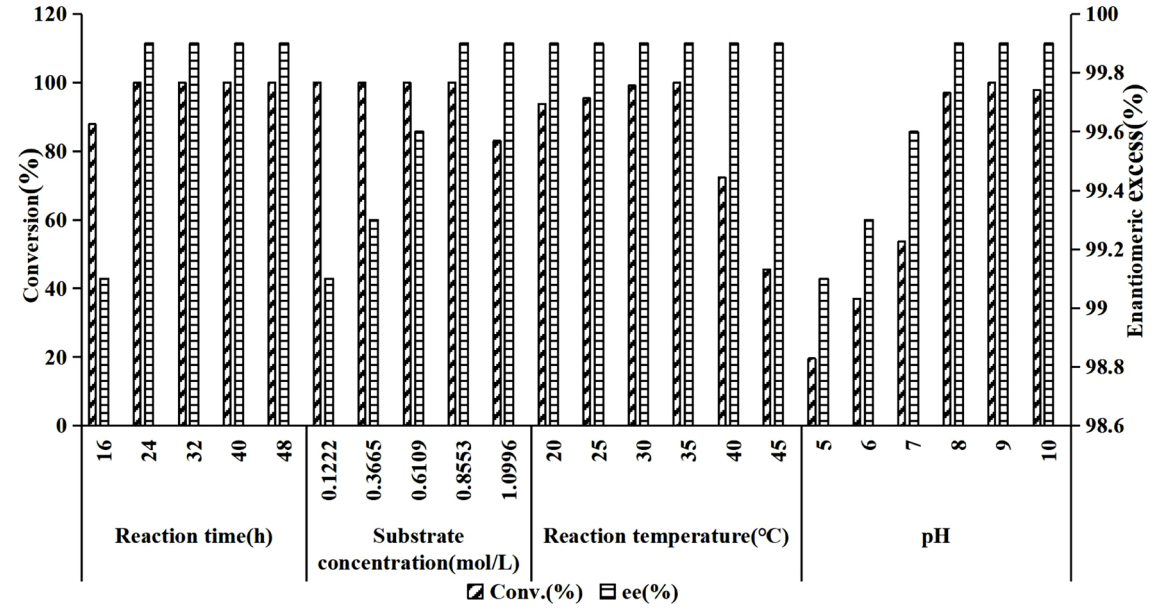

Fig. 7. Effect of reaction condition on batch reduction in the shaker.

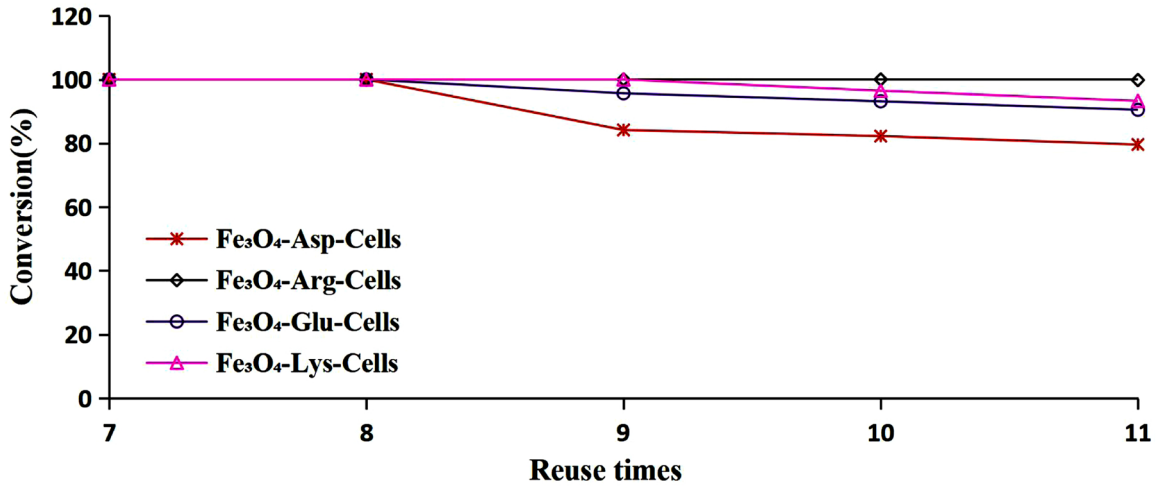

Fig. 8. Reuse of immobilized cells for batch reduction in the shaker.

3.3.3. Effect of temperature on reduction

Fig. 7 indicated that conversion increased with the increase of temperature at 20–35 ℃ and decreased at above 35 ℃. The optimal reduction temperature was 35 ℃. Enzyme activity was lost or inhibited at high temperatures due to protein denaturation. For the Fe_3O_4-Arg-Cells catalyst, the temperature had little effect on the enantiomeric excess of (*R*)-CHBE, which remained above 99.9 %.

3.3.4. Effect of buffer pH on reduction

The stable catalytic activity of Fe_3O_4-Arg-Cells was observed at pH 8–10 in Fig. 7. At pH 5–9, the conversion gradually increased with the increase of pH until the maximum conversion reached 100 %. 100 % conversion was achieved at pH 9 while conversion was only 53.71 % at pH 7. The optimal reduction pH was pH 9. Arginine is a basic amino acid. The dissociation state of arginine is affected by the pH value of the buffer solution. Therefore, the catalytic activity of Fe_3O_4-Arg-Cells was also affected by the pH of the buffer. The enantiomeric excess of (*R*)-CHBE was not affected by the pH of the buffer and was maintained above 99 %.

3.4. Reuse of Fe_3O_4-Arg-Cells in the batch reduction in a shaker

Fe_3O_4-Arg-Cells can be recovered by an external magnetic field and reused easily in reduction. Fig. 8 indicated that Fe_3O_4-Arg-Cells reused 11 times achieved 99.8 % conversion. The enantiomeric excess of (*R*)-CHBE was maintained above 99 % in the reduction with reused Fe_3O_4-Arg-Cells as catalysts. The reuse of Fe_3O_4-Arg-Cells was a powerful method for the asymmetric reduction of COBE; it can enhance productivity improvement.

3.5. Optimization of batch reduction reaction conditions under alternating magnetic field

3.5.1. Effect of magnetic field strength on the batch reduction in the alternating magnetic field

Fig. 9 demonstrated that with the Fe_3O_4-Arg-Cells as catalysts, conversion increased initially and then decreased with increasing magnetic field intensity. The alternating magnetic field can accelerate the movement of Fe_3O_4-Arg-Cells to improve the reaction rate of reduction. When the magnetic field strength was less than 12 Gs, Fe_3O_4-

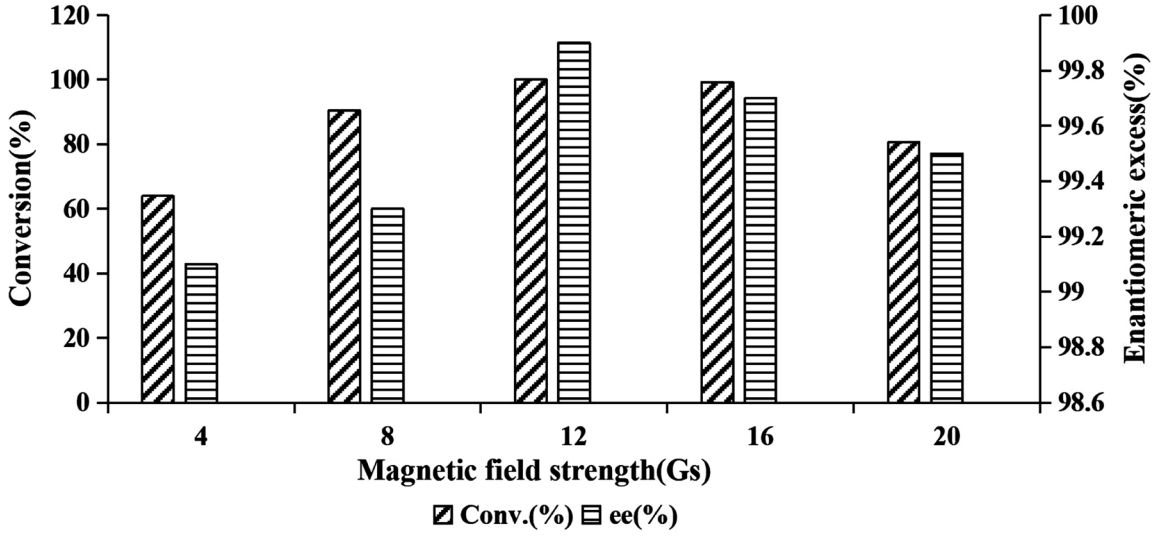

Fig. 9. Effect of magnetic field strength on reduction.
(Magnetic field frequency 500 Hz, Reaction time 8 h).

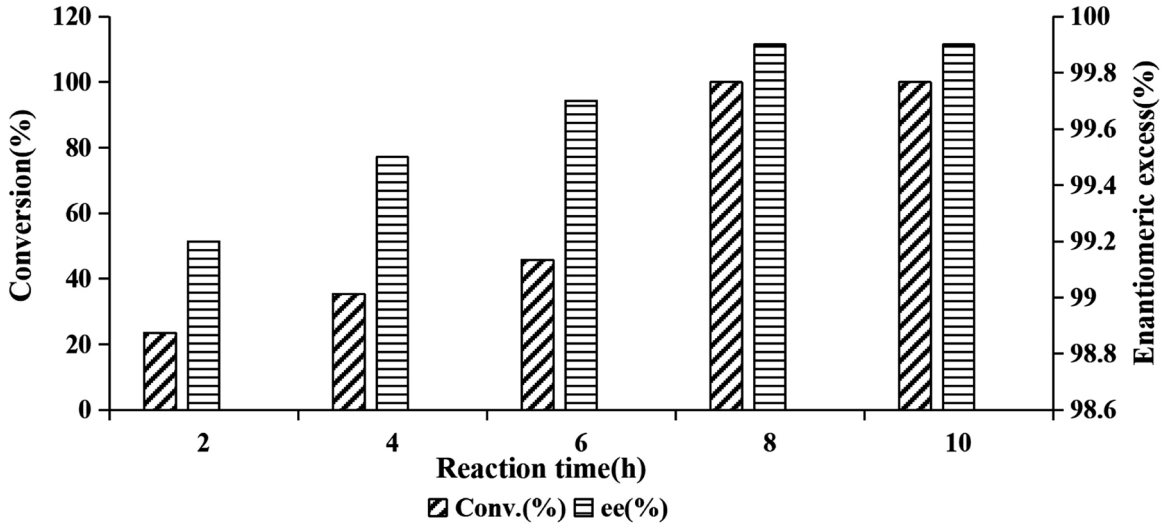

Fig. 10. Effect of reaction time on reduction in alternating magnetic field.
(Magnetic field frequency 500 Hz, Magnetic field strength 12 Gs).

Arg-Cells were in an activated state and the conversion increased with the increase of the magnetic field strength. However, when the magnetic field intensity exceeded 12 Gs, the conversion started to decrease. Fe_3O_4-Arg-Cells generated an induced magnetic field under the action of the external magnetic field. The interaction between these magnetic fields affected the spatial conformation of the enzyme and brought about changes in the activity of Fe_3O_4-Arg-Cells. The enantiomeric excess of (*R*)-CHBE was above 99 % under different magnetic field strengths. The optimal magnetic field frequency and magnetic field intensity were determined to be 500 Hz and 12 Gs, respectively.

3.5.2. Effect of reaction time on the batch reduction in the alternating magnetic field

Under the same condition, 0.8553 mol/L COBE can be converted completely in 8 h in the alternating magnetic field, while in the shaker for 24 h. Fe_3O_4-Arg-Cells were uniformly distributed in the alternating magnetic field; they could sufficiently make contact with the COBE solution and mass transfer was not required by shaking and stirring. The reaction time was remarkably shortened and the conversion efficiency was greatly improved. The specific results were shown in Fig. 10.

3.6. Continuous reduction reaction in a magnetic fluidized bed reactor system (MFBRS)

MFBRS is considered an efficient system when coupled with magnetic immobilized cells or enzymes for biocatalysis and biotransformation process intensification [39,40].

3.6.1. Effect of substrate flow rate on reduction reaction in MFBRS

Fig. 11 indicated that the conversion gradually decreased with the increase of substrate flow rate because of the insufficient retention time in which the substrate molecule stayed in the reactor. When the substrate flow rate increased from 25 μL/min to 200 μL/min, the conversion decreased from 100 % to 38.93 % and the enantiomeric excess of (*R*)-CHBE was above 99.0 %. Therefore, the optimal substrate flow rate was 25 μL/min.

3.6.2. Effect of substrate concentration on reduction in MFBRS

Fig. 12 revealed that the conversion decreased with the increase of substrate concentration. The enantiomeric excess of (*R*)-CHBE remained above 99 %. The active site of the cell was not fully saturated

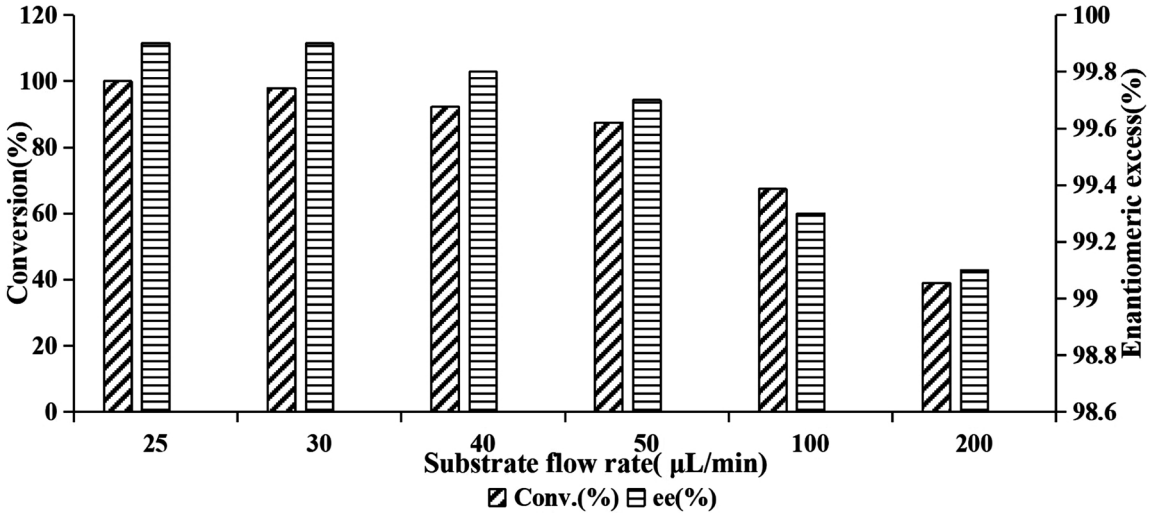

Fig. 11. Effect of substrate flow rate on reduction in magnetic fluidized bed reactor.
(Magnetic field strength 12 Gs, Reaction time 6 h, Temperature 35 ℃, Substrate concentration 1.5882 mol/L).

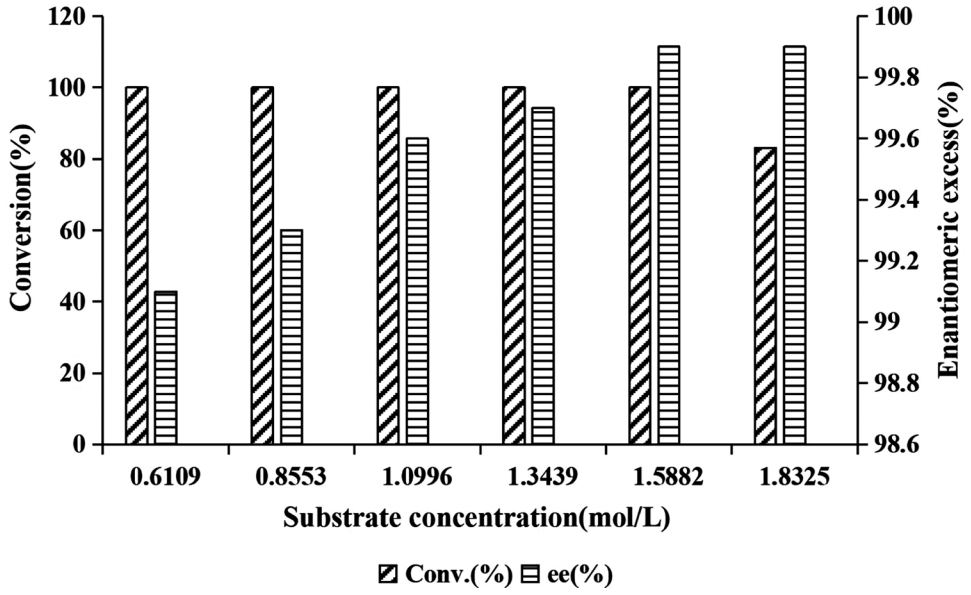

Fig. 12. Effect of substrate concentration on reduction in magnetic fluidized bed reactor.
(Magnetic field strength 12 Gs, Reaction time 6 h, Temperature 35 ℃, Substrate flow rate 25 μL/min).

Table 2
Optimal reduction condition in different three systems.

	Batch reaction in shaker	Batch reaction in magnetic field	Continuous reaction in magnetic field
Optimal substrate concentration(mol/L)	0.8553	0.8553	1.5882
Optimal reaction time(h)	24	8	6
Substrate volume(mL)	1	1	10
conversion(%)	100	100	100
Enantiomeric excess of (*R*)-CHBE(%)	99.9	99.9	99.9
Productivity(mmol/h)	0.392	1.176	2.647

and its catalytic activity was not fully exploited at low substrate concentrations. The number of COBE molecules in contact with Fe_3O_4-Arg-Cells increased with the substrate concentration increase indicating that the conversion of COBE probably increased. During the continuous transformation, the substrate concentration increase could maximize the use of the catalyst within a certain range and probably reduced the conversion because of high substrate concentration inhibition.

3.7. Comparison of optimization results of the three systems

Productivity was defined as conversion per unit time. Table 2 revealed the detailed productivities of batch reduction in the shaker, batch reduction in the alternating magnetic field, and continuous reduction in MFBRS. MFBRS is considered an efficient system for intensification of biocatalysis and biotransformation processes using magnetically immobilized cells (Fe_3O_4-AA-Cells) as a catalyst. The

productivity of continuous reaction in the magnetic field was much higher than the other two systems; this provides insights for the efficient production of (*R*)-CHBE.

4. Conclusion

Magnetic carriers are of interest because of their small particle size, superparamagnetism, low toxicity, and easy separation from the system through external magnetic fields. In our study, an alternating magnetic field reactor was used in 1.5882 mol/L COBE continuous reduction for preparing (*R*)-CHBE. The conversion and enantiomeric excess of (*R*)-CHBE were 100 % and > 99.9 %, respectively. The substrate treatment capacity noted in this study is a great breakthrough compared to previous studies.

Fe_3O_4-Arg-Cells were used as a catalyst in the reduction in a shaker. Under the optimal conditions in a shaker (substrate concentration 0.8553 mol/L, 35 °C, pH 9, 24 h), 100 % and 99.9 % respectively of the (*R*)-CHBE conversion and enantiomeric excess (e.e.) was achieved. Fe_3O_4-Arg-Cells reused 11 times in the shaker indicated achieved a 99.8 % conversion. The enantiomeric excess of (*R*)-CHBE was maintained above 99 % in the reduction process with reused Fe_3O_4-Arg-Cells as catalysts.

Fe_3O_4-Arg-Cells were used in the batch reduction under an alternating magnetic field and continuous reduction in an MFBRS. Under the optimal conditions of the two reaction systems, 100 % and 99.9 % respectively of the (*R*)-CHBE conversion and enantiomeric excess was achieved. Continuous reduction in MFBRS displayed greater productivity reduction. MFBRS is an efficient system for the intensification of biocatalysis and biotransformation processes. This study provides a new basis for further research on the application of immobilization technology to improve the stereoselectivity of yeast in the asymmetric reduction of carbonyl compounds. Amino acid-modified magnetic immobilized cells can greatly enhance the efficiency of asymmetric reduction reaction in MFBRS.

CRediT authorship contribution statement

Hongqian Dai: Writing - original draft. **Hanbing Shi:** Writing - original draft. **Lan Tang:** Writing - review & editing. **Xingyuan Sun:** Writing - review & editing. **Zhimin Ou:** Conceptualization, Methodology.

Declaration of Competing Interest

The authors report no declarations of interest.

Acknowledgements

We thank the National Nature Science Foundation of China (21978267) and the Natural Science Foundation of Zhejiang Province (LY15B060005, LY15B060007) for the financial support.

Appendix A. Supplementary data

Supplementary material related to this article can be found, in the online version, at doi:https://doi.org/10.1016/j.procbio.2020.07.027.

References

[1] R.N. Patel, Biocatalysis: synthesis of key intermediates for development of pharmaceuticals, ACS Catal. 1 (2011) 1056–1074, https://doi.org/10.1021/cs200219b.
[2] R.Y. Guo, Y. Nie, X.Q. Mu, Y. Xu, R. Xiao, Genomic mining-based identification of novel stereospecific aldo-keto reductases toolbox from *Candida parapsilosis* for highl-y enantioselective reduction of carbonyl compounds, J Mol Catal B: Enzym. 105 (2014) 66–73, https://doi.org/10.1016/j.molcatb.2014.04.003.
[3] P. Kluson, P. Stavarek, V. Penkavova, H. Vychodilova, S. Hejda, N. Jaklova, P. Curin-ova, Stereoselective synthesis of optical isomers of ethyl 4-chloro-3-hydroxybutyrate i-n a microfluidic chip reactor, J. Flow Chem. 9 (2019) 221–230, https://doi.org/10.1007/s41981-019-00043-y.
[4] J. Kasprzak, F. Bischoff, M. Rauter, K. Becker, K. Baronian, R. Bode, F. Schauer, H.M. Vorbrodt, G. Kunze, Synthesis of 1-(*S*)-phenylethanol and ethyl (*R*)-4-chloro-3-hydroxybutanoate using recombinant *Rhodococcus* erythropolis alcohol dehydrogenase pro-duced by two yeast species, Biochem. Eng. J. 106 (2016) 107–117, https://doi.org/10.1016/j.bej.2015.11.007.
[5] Y.C. He, D.P. Zhang, Z.C. Tao, X. Zhang, Z.X. Yang, Discovery of a reductase-producing strain recombinant *E. coli* CCZU-A13 using colorimetric screening and its whol-e cell-catalyzed biosynthesis of ethyl (*R*)-4-chloro-3-hydroxybutanoate, Bioresource Technol. 172 (2014) 342–348, https://doi.org/10.1016/j.biortech.2014.09.062.
[6] Q. Xu, W.Y. Tao, H. Huang, S. Li, Highly efficient synthesis of ethyl (*S*)-4-chloro-3-hydroxybutanoate by a novel carbonyl reductase from *Yarrowia lipolytica* and using mannitol or sorbitol as cosubstrate, Biochem. Eng. J. 106 (2016) 61–67, https://doi.org/10.1016/j.bej.2015.11.010.
[7] Y.C. He, D.P. Zhang, J.H. Di, Y.Q. Wu, Z.C. Tao, F. Liu, Z.J. Zhang, G.G. Chong, Y. Ding, C.L. Ma, Effective pretreatment of sugarcane bagasse with combination pretreatment and its hydrolyzates as reaction media for the biosynthesis of ethyl (*S*)-4-chloro-3-hydroxybutanoate by whole cells of *E. coli* CCZU-K14, Bioresource Technol. 211 (2016) 720–726, https://doi.org/10.1016/j.biortech.2016.03.150.
[8] L.F. Chen, H.Y. Fan, Y.P. Zhang, W. Wei, J.P. Lin, D.Z. Wei, H.L. Wang, Enhancement of ethyl (*S*)-4-chloro-3-hydroxybutanoate production at high substrate concentration by in situ resin adsorption, J. Biotechnol. 251 (2017) 68–75, https://doi.org/10.1016/j.jbiotec.2017.04.014.
[9] Y. Dai, B. Huan, H.S. Zhang, Y.C. He, Effective biotransformation of ethyl 4-chloro-3-oxobutanoate into ethyl (*S*)-4-chloro-3-hydroxybutanoate by recombinant *E. coli* CCZU-T15 whole cells in [ChCl][Gly]-water media, Appl. Biochem. Biotechnol. 181 (2017) 1347–1359, https://doi.org/10.1007/s12010-016-2288-0.
[10] X. Liu, R. Chen, Z.W. Yang, J.L. Wang, J.P. Lin, D.Z. Wei, Characterization of aputative stereoselective oxidoreductase from *gluconobacter oxydans* and its applicatio-n in producing ethyl (*R*)-4-chloro-3-hydroxybutanoate ester, Mol. Biotechnol. 56 (2014) 285–295, https://doi.org/10.1007/s12033-013-9707-z.
[11] C.X. Ning, E.Z. Su, D.Z. Wei, Characterization and identification of three novel aldo-keto reductases from *Lodderomyces elongisporus* for reducing ethyl 4-chloroacetoacetate, Arch. Biochem. Biophys. 564 (2014) 219–228, https://doi.org/10.1016/j.abb.2014.10.007.
[12] Q.Y. Wang, T.T. Ye, Z.Z. Ma, R. Chen, T. Xie, X.P. Yin, Characterization and site-directed mutation of a novel aldo-keto reductase from *Lodderomyces elongisporus* NRRL YB-4239 with high production rate of ethyl (*R*)-4-chloro-3-hydroxybutanoate, J. Ind. Microbiol. Biotechnol. 41 (2014) 1609–1616, https://doi.org/10.1007/s10295-014-1502-8.
[13] Y. Ni, C.X. Li, L.J. Wang, J. Zhang, J.H. Xu, Highly stereoselective reduction of prochiral ketones by a bacterial reductase coupled with cofactor regeneration, Org. Biomol. Chem. 9 (2011) 5463–5468, https://doi.org/10.1039/C1OB05285C.
[14] X. Chen, Z.Q. Liu, C.P. Lin, Y.G. Zheng, Efficient biosynthesis of ethyl (*R*)-4-chloro-3-hydroxybutyrate using a stereoselective carbonyl reductase from *Burkholderia gladioli*, BMC Biotechnol. 16 (2016) 70, https://doi.org/10.1186/s12896-016-0301-x.
[15] Y.C. He, Z.C. Tao, J.H. Di, L. Chen, C.L. Ma, Effective symmetric bioreduction of ethyl 4-chloro-3-oxobutanoate to ethyl (*R*)-4-chloro-3-hydroxybutanoate by recombinant *E. coli* CCZU-A13 in [Bmim]PF6-hydrolyzate media, Bioresource Technol. 214 (2016) 411–418, https://doi.org/10.1016/j.biortech.2016.04.134.
[16] P. Wei, J.X. Gao, G.W. Zheng, H. Wu, W.Y. Lou, Engineering of a novel carbonyl reductase with coenzyme regeneration in *E. coli* for efficient biosynthesis of enantiopure chiral alcohols, J. Biotechnol. 230 (2016) 54–62, https://doi.org/10.1016/j.jbiotec.2016.05.004.
[17] Y.P. Zhang, H.L. Wang, L.F. Chen, K. Wu, D.Z. Wei, Efficient production of ethyl (*R*)-4-chloro-3-hydroxybutanoate by a novel alcohol dehydrogenase from *Lactobacillus curieae* S1L19, J. Mol. Catal. B-Enzym. 134 (2016) 51–60, https://doi.org/10.1016/j.molcatb.2016.09.010.
[18] G.G. Chong, J.H. Di, C.L. Ma, D.J. Wang, C. Wang, L.L. Wang, P.Q. Zhang, J. Zhu, Y.C. He, Enhanced bioreduction synthesis of ethyl (*R*)-4-chloro-3-hydroxybutanoate by alkalic salt pretreatment, Bioresource Technol. 261 (2018) 196–205, https://doi.org/10.1016/j.biortech.2018.04.015.
[19] T. Gu, B.Q. Wang, Z.W. Zhang, Z.T. Wang, G.G. Chong, C.L. Ma, Y.J. Tang, Y.C. He, Sequential pretreatment of bamboo shoot shell and biosynthesis of ethyl (*R*)-4-chloro-3-hydroxybutanoate in aqueous-butyl acetate media, Process Biochem. 80 (2019) 112–118, https://doi.org/10.1016/j.procbio.2019.02.002.
[20] X. Xu, Y. Cai, Z. Song, X. Qiu, J. Zhou, Y. Liu, T. Mu, D. Wu, Y. Guan, J. Xing, Desulfurization of immobilized sulfur-oxidizing bacteria, *Thialkalivibrio versutus*, by magnetic nanaoparticles under haloalkaliphilic conditions, Biotechnol. Lett. 37 (2015) 1631–1635, https://doi.org/10.1007/s10529-015-1845-x.
[21] J. Hou, F. Liu, N. Wu, J. Ju, B. Yu, Efficient biodegradation of chlorophenols in aqueous phase by magnetically immobilized aniline-degrading *Rhodococcus rhodochrous* strain, J. Nanobiotechnol. 14 (2016) 5, https://doi.org/10.1186/s12951-016-0158-0.
[22] P.F. Sun, C. Hui, S. Wang, R.A. Khan, Q.C. Zhang, Y.H. Zhao, Enhancement of algicidal properties of immobilized *Bacillus methylotrophicus* ZJU by coating with magnetic Fe_3O_4 nanoparticles and wheat bran, J. Hazard. Mater. 301 (2016) 65–73, https://doi.org/10.1016/j.jhazmat.2015.08.048.
[23] A. Ebrahiminezhad, V. Varma, S. Yang, A. Berenjian, Magnetic immobilization of *Bac-illus subtilis* natto cells for menaquinone-7 fermentation, Appl. Microbiol. Biotechnol. 100 (2016) 173–180, https://doi.org/10.1007/s00253-015-6977-3.
[24] R.Y. Li, G.M. Fu, C.M. Liu, D.J. McClements, Y. Wan, S.M. Wang, T. Liu, Tannase immobilisation by amino-functionalised magnetic Fe_3O_4-chitosan nanoparticles and

its application in tea infusion, Int. Biol. Macromol. 114 (2018) 1134–1143, https://doi.org/10.1016/j.ijbiomac.2018.03.077.
[25] J. Zhao, M. Lin, G. Chen, Facile recycling of *Escherichia coli* and *Saccharomyce-s cerevisiae* cells from suspensions using magnetic modification method and mechanism analysis, Colloid Surf. B 169 (2018) 1–9, https://doi.org/10.1016/j.colsurfb.2018.05.006.
[26] M.M. Seifi, E. Iranmanesh, M.A. Asadollahi, A. Arpanaei, Biotransformation of benzaldehyde into l-phenylacetylcarbinol using magnetic nanoparticles-coated yeast cells, Biotechnol. Lett. 42 (2020) 597–603, https://doi.org/10.1007/s10529-020-02798-0.
[27] H. Ghorbannezhad, H. Moghimi, R.A. Taheri, Enhanced biodegradation of phenol by magnetically immobilized *Trichosporon cutaneum*, Ann. Microbiol. 68 (2018) 485–491, https://doi.org/10.1007/s13213-018-1353-z.
[28] Y.P. Zang, N. Guo, J. Jiao, X.Q. Wang, Q.Y. Gai, W.J. Xu, Y.J. Fu, Application of magnetically immobilized edible fungus for the biotransformation of panax notoginseng saponin Rbl to Rd and Rg3, J. Chromatogr. B 1061 (2017) 306–313, https://doi.org/10.1016/j.jchromb.2017.07.038.
[29] Y.J. Jin, F. Liu, C. Shan, M.P. Tong, Y.L. Hou, Efficient bacterial capture with amino acid modified magnetic nanoparticles, Water Res. 50 (2014) 124–134, https://doi.org/10.1016/j.watres.2013.11.045.
[30] Z.M. Ou, J.Y. Pan, L. Tang, H.B. Shi, Continuous enantiomer-selective acylation reaction of 1-phenylethanamine in a magnetic fluidized bed reactor system (MFBRS), J. Chem. Technol. Biotechnol. 94 (2019) 1951–1957, https://doi.org/10.1002/jctb.5978.
[31] J.Y. Park, E.S. Choi, M.J. Baek, G.H. Lee, Colloidal stability of amino acid coated magnetite nanoparticles in physiological fluid, Mater. Lett. 63 (2009) 379–381, https://doi.org/10.1016/j.matlet.2008.10.057.
[32] A. Ebrahiminezhad, Y. Ghasemi, S. Rasoul-Amini, J. Barar, S. Davaran, Impact of amino-acid coating on the synthesis and characteristics of iron-oxide nanoparticles (IONs), Bull. Korean Chem. Soc. 33 (2012) 3957–3962, https://doi.org/10.5012/bkcs.2012.33.12.3957.
[33] L. Bromberg, E.P. Chang, T.A. Hatton, et al., Bactericidal core-shell paramagnetic nanoparticles functionalized with poly(hexamethylene biguanide), Langmuir 27 (2011) 420–429, https://doi.org/10.1021/la1039909.
[34] J.Y. Pan, Z.M. Ou, L. Tang, H.B. Shi, Enhancement of catalytic activity of lipase-immobilized Fe_3O_4-chitosan microsphere for enantioselective acetylation of racemic 1-phenylethylamine, Korean J. Chem. Eng. 36 (2019) 729–739, https://doi.org/10.1007/s11814-019-0249-3.
[35] K. Can, M. Ozmen, M. Ersoz, Immobilization of albumin on aminosilane modified superparamagnetic magnetite nanoparticles and its characterization, Colloid Surf. B 71 (2009) 154–159, https://doi.org/10.1016/j.colsurfb.2009.01.021.
[36] I. Antal, M. Koneracka, M. Kubovcikova, V. Zavisova, I. Khmara, D. Lucanska, L. Jelenska, I. Vidlickova, M. Zatovicova, S. Pastorekova, D,L-lysine functionalized Fe_3O_4 nanoparticles for detection of cancer cells, Colloids Surf. B Biointerfaces 163 (2018) 236–245, https://doi.org/10.1016/j.colsurfb.2017.12.022.
[37] B. Hu, J. Pan, H.L. Yu, J.W. Liu, J.H. Xu, Immobilization of Serratia marcescens lipase onto amino-functionalized magnetic nanoparticles for repeated use in enzymatic synthesis of Diltiazem intermediate, Process. Biochem. 44 (2009) 1019–1024, https://doi.org/10.1016/j.procbio.2009.05.001.
[38] B. Unal, Z. Durmus, A. Baykal, H. Sozeri, M.S. Toprak, L. Alpsoy, L-histidine coated iron oxide nanoparticles: synthesis, structural and conductivity characterization, J. Alloys Compd. 505 (2010) 172–178, https://doi.org/10.1016/j.jallcom.2010.06.022.
[39] M. Hajar, F. Vahabzadeh, Biolubricant production from castor oil in a magnetically stabilized fluidized bed reactor using lipase immobilized on Fe_3O_4 nanoparticles, Ind. Crop Prod. 94 (2016) 544–556, https://doi.org/10.1016/j.indcrop.2016.09.030.
[40] K.J. Dussan, O.R. Justo, V.H. Perez, G.F. David, E.G. Silveira, S.S. da Silva, Bioethanol production from sugarcane bagasse hemicellulose hydrolysate by immobilized *S. shehatae* in a fluidized bed fermenter under magnetic field, Bioenerg. Res. 12 (2019) 338–346, https://doi.org/10.1007/s12155-019-09971-y.